Nanoscale

Cite this: DOI: 10.1039/c2nr30162h

www.rsc.org/nanoscale

COMMUNICATION

Scanning tunnelling microscopy of suspended graphene

Recep Zan,*[ab] Chris Muryn,[c] Ursel Bangert,[b] Philip Mattocks,[d] Paul Wincott,[e] David Vaughan,[e] Xuesong Li,[fg] Luigi Colombo,[h] Rodney S. Ruoff,[f] Bruce Hamilton[d] and Konstantin S. Novoselov[a]

Received 19th January 2012, Accepted 21st March 2012
DOI: 10.1039/c2nr30162h

Suspended graphene has been studied by STM for the first time. Atomic resolution on mono- and bi-layer graphene samples has been obtained after ridding the graphene surface of contamination *via* high-temperature annealing. Static local corrugations (ripples) have been observed on both types of structures.

Graphene offers new, unexplored opportunities in surface science: it is a rare case of surface without a bulk, so the methods of surface science give us unique information about this material. Scanning tunnelling microscopy (STM), in particular, is a powerful technique for studying surface morphology as well as electronic structure on the atomic scale. STM studies of graphene have been carried out for materials prepared on a number of substrates such as SiO_2, SiC, Cu, Ir, Ru and others.[1–8] The graphene layers prepared on these substrates were obtained by different techniques, for example by exfoliation,[9] chemical vapour deposition (CVD) using different types of gases (*e.g.*, methane or ethylene) on different substrates,[10–12] as well as by graphitization of SiC.[13] Characterization of such films has typically exploited Z-imaging scanning tunnelling spectroscopy (STS) and low energy diffraction pattern analysis, all *in situ* and in UHV. Initial reports involved pure graphene,[1–5,7] but STM analysis of metal clusters on graphene has also been performed, exploiting the crystallographic quality and chemical stability of graphene as a substrate for cluster measurement.[1,8,14,15] Graphene was also studied on graphite *via* STM where graphene flakes had decoupled from the substrate and showed the characteristic behaviour of monolayer graphene.[6] Geringer *et al.*[16] claimed that quasi-suspended graphene was studied since the roughness of the SiO_2 substrate is higher than that of the graphene on top of it, implying that some areas of the graphene do not touch the surface, and hence suspended regions are present. Luican *et al.*[17] have also recently attempted to study graphene on transmission electron microscopy (TEM) grids using STM; they have imaged graphene layers on non-suspended parts of the sample, *i.e.*, on grid bars, but they were unable to image suspended regions of graphene because they consisted of relatively large areas, causing excessive spatial fluctuations for STM imaging, even at 4 K. Truly suspended graphene has so far been studied mainly in TEM.[18,19] Both theory[20,21] and experiment[8,22] suggest that the substrates on which graphene is typically deposited, for characterisation and for applications, have a significant influence on its properties. Because of this and because of uncertainties concerning the invasiveness of TEM or STEM experiments as a result of the high energy density of the electron beam even at energies below the displacement threshold of carbon atoms in graphene (*i.e.* <80 keV),[23,24] we have attempted STM z-image studies of freely suspended graphene. Here we present for the first time examples of atomic scale resolution imaging of freely suspended graphene layers which point to the conclusion that nanoscale, temporally static ripples can be reproducibly observed, at least with the preparation and suspension methods described. The ability to obtain such data rests largely on *in situ* cleaning procedures used, which we also outline in this paper.

The graphene samples used in this experiment were grown by chemical vapour deposition (CVD) onto copper substrates.[11] The graphene on Cu was then spin-coated with poly-methyl methacrylate (PMMA) to provide mechanical support and to facilitate handling after Cu substrate removal. The Cu substrate was etched away in a 0.1 molar ammonium persulfate ($(NH_4)_2S_2O_8$) solution, rinsed in deionised water, and then transferred to a 400 mesh lacey-carbon-coated Cu grid. The lacey carbon network coating consists of narrow (50 nm) interconnected strips of amorphous carbon bordering holes of a few microns in diameter, providing a predominantly open structure, thus giving rise to suspended graphene over about 90% of the area. The fact that the suspended parts are only a few microns in diameter and measurements were conducted in the proximity of the grid bar helped ensure the mechanical stability of the graphene on the carbon coated Cu grid during the experiment. The PMMA was subsequently dissolved by immersion in acetone for a few minutes. The TEM grid was then dried in a critical point dryer to avoid collapse or deformation of the membranes due to surface tension. The transfer of graphene involves chemical treatment, and so

[a]*School of Physics and Astronomy, The University of Manchester, Manchester, M13 9PL, UK. E-mail: recepzan@gmail.com; Tel: +44 (0) 161 306 2255*
[b]*School of Materials, The University of Manchester, Manchester, M13 9PL, UK*
[c]*School of Chemistry, The University of Manchester, Manchester, M13 9PL, UK*
[d]*Photon Science Institute, The University of Manchester, Manchester, M13 9PL, UK*
[e]*School of Earth, Atmospheric and Environmental Sciences, The University of Manchester, Manchester, M13 9PL, UK*
[f]*Department of Mechanical Engineering and the Materials Science and Engineering Program, The University of Texas at Austin, Austin, TX, 78712, USA*
[g]*IBM, T.J. Watson Research Center, Yorktown, NY, USA*
[h]*Texas Instruments Incorporated, Dallas, TX 75243, USA*

residues, *e.g.*, PMMA and other unintentional impurities, may be left on the graphene surface, which affect the imaging conditions in the STM. In fact, introduction of chemical surface contamination at some level is common for all film transfer or processing steps, *e.g.* similar residues are likely to form as a result of lithographic procedures when defining contacts or mesa structure on graphene on nonconductive surfaces like SiO_2.

Both UHV RHK and Omicron low-temperature UHV STM systems (residual pressure 10^{-10} mbar) and electrochemically etched tungsten tips, formed and cleaned in UHV, were used to analyze the surface of graphene in our experiments. All STM data were taken at room temperature (300 K) and sample–tip bias voltages were typically between 0.5 V and 1.5 V with tunnel currents ranging from 0.1 nA to 1.0 nA; for atomic resolution a higher tunnelling current was used. To ensure optimised tip performance, gold on mica and graphite (HOPG) samples were used as references. Also, in order to ensure that tunnelling was occurring on the suspended parts, we systematically took images at small spatial separations across entire grid squares with all high quality images yielding a similar result, which was repeated on a number of different samples. In the following we demonstrate an annealing process to minimize residue on the suspended graphene, as well as hexagonal and triangular atomic structure and topographic ripples. The experimental data were analysed by using WSxM software.[25]

Prior to mounting the TEM grid in the STM chamber, we ascertained the presence of graphene flakes and their coverage in the TEM, and ensured, *via* electron diffraction, that the deposited material was predominantly monolayer graphene: the films we used also showed the presence of bilayer regions over less than 5% of the sample area. Unfortunately most of the area was covered with polymeric, hydrocarbon residue, from, *e.g.*, the PMMA, as described above as a result of wet chemistry, consisting of carbon, oxygen and hydrogen, as revealed by our EDS and EELS measurements. This residue sometimes forms randomly oriented thick amorphous layers. The residue also contains metal impurities from the growth substrate *e.g.*, Cu, and inevitably Si, a well known impurity on graphene regardless of the production method. Thus only small, nanometre scale clean patches exist on the untreated graphene surface, as is commonly observed in TEM studies,[24] (Fig. 1(a)). Better surface preparation techniques will have to be employed to have access to residue free graphene.

Since we observed surface contamination, principally consisting of hydrocarbons, on the graphene surface by TEM, we annealed the graphene in both TEM and STM in UHV environment at various temperatures, ranging from 50 °C to 550 °C in an attempt to find the best conditions to achieve stable tunnelling and good image quality. Fig. 1 shows TEM and STM images of suspended graphene before and after annealing; these indicate the presence of residue (Fig. 1(a) and (c)) and effects of annealing at elevated temperatures (Fig. 1(b) and (d)). It is clear from both TEM and STM images that annealing at 550 °C shows the cleanest surface and stable tunnelling in STM.

By further exploring the annealing regimes in terms of time and temperature it was found that annealing for 24 hours at 500 °C is usually sufficient to remove almost all organic (hydrocarbon) contamination, so that the size of the clean graphene patches increased from few nm^2 to several hundreds of nm^2 (see the inset of Fig. 1(b)), and with a well formed tip we were able to obtain atomic resolution images (Fig. 2).

A clear honeycomb monolayer structure was observed with an interatomic distance of 1.4 Å, consistent with literature values.

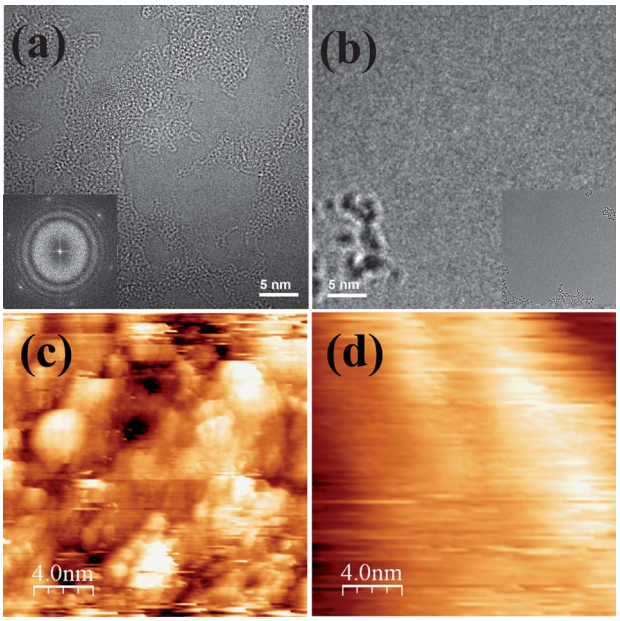

Fig. 1 TEM images of suspended graphene (a) before annealing with FFT shown in the inset; (b) after annealing at 550 °C for a few hours, a low magnification image shown in the inset (700 nm^2 frame); STM images (c) before annealing and (d) after annealing at 550 °C. All images represent raw data. The STM scanning conditions were: tunnelling voltage of 0.5–1.5 V, current 0.1–1 nA.

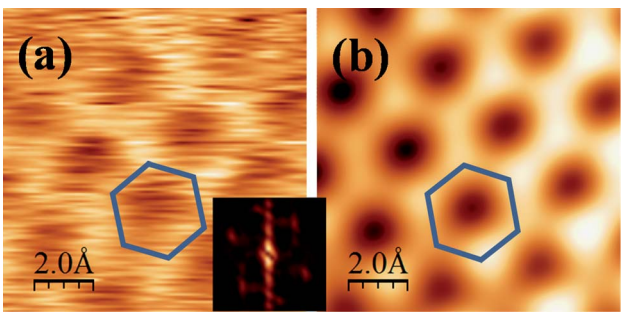

Fig. 2 High resolution STM images of monolayer graphene. (a) Raw and (b) FFT filtered image. A hexagonal monolayer structure can be observed in both images. The image acquisition parameters were: V_{bias} = +0.6 V and I = 0.3 nA. The inset shows the FFT.

Consequently Fig. 2(a) shows six spots in the Fourier transform (inset), indicative of the graphene lattice. This cleaning procedure allowed us to acquire atomic resolution graphene images at almost every probing position on the suspended layer.

In some areas of the sample both hexagonal and triangular structures were observed in a single image frame, corresponding to monolayer and bilayer graphene respectively, as shown by the raw and FFT filtered images of such regions in Fig. 3(a) and (b), respectively.

The stability of 2-D structures has long been debated,[26,27] and ripples in graphene layers, although commonly imaged in supported films,[2,4,16] are of great interest. Their origin, whether they are intrinsically driven by energy minimisation of the 2-D structure[28] or are rather due to essentially extrinsic phenomena, has not been resolved in the existing literature. Many such extrinsic causes could exist

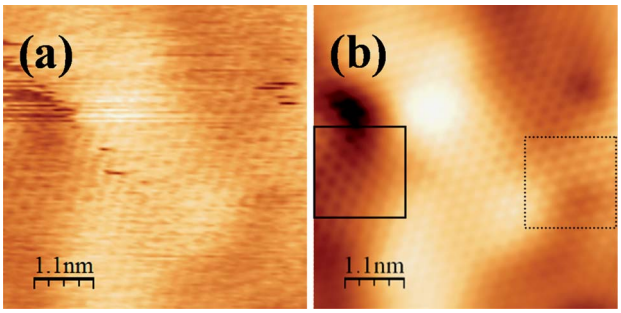

Fig. 3 High resolution monolayer and bilayer graphene region. (a) Raw and (b) FFT filtered images. Hexagonal monolayer (solid line square) and triangular bilayer (dotted line square) structures can be observed in both images. The image acquisition parameters were: $V_{bias} = +0.6$ V and $I = 0.5$ nA.

depending on sample preparation *e.g.* defect mediated local changes in graphene stiffness, unintentional bending of a supporting grid or mechanical strain during fabrication.[29] Equally, the question as to whether these ripples are dynamic or static is a subject of great interest and is hitherto unresolved. In a previous STEM study,[30] using Fourier filtering procedures, we have shown that ripples in monolayer graphene have wavelengths on the scale of 5 to 10 nm, and amplitudes of typically 0.5 nm. Ripple patterns observed in the STEM have proven to change in subsequent scans, being strongly influenced by the time varying point defect distribution which is driven by the electron beam interactions with the film. In the present STM images of suspended graphene we observe distinct topographic ripple features, which strongly resemble the ripples of STEM data in terms of shape, wavelength and height. We have systematically imaged graphene addressing many different areas of suspended material, and conducting repeat scans in given areas. In doing so we established the general topography and also the stability of ripples in suspended graphene; examples are given in Fig. 4(a) and (b), where height variations (ripple amplitude) of the order of 1 nm were observed. A line profile (blue dotted line in Fig. 4(b)) shows the height variation across a 10 nm frame size in the inset Fig. 4(b). The images in Fig. 4(a) and (b) represent the first and last in a long sequence of repeated imaging. The ripples are stable, *i.e.* no changes, aside from small sample drift, are detected over a time period of about 5 minutes of continuous imaging. The same situation, on a magnified scale, is evident in Fig. 4(c) and (d), showing a different area of graphene. Again, the images in Fig. 4(c) and (d) are the first and the last of a series. The ripple amplitude here is about 4 Å, which can be seen from the line profile shown in the inset. In both sets of images (a, b and c, d) the lateral periodicity or wavelength of the ripples is a few (~5) nm.

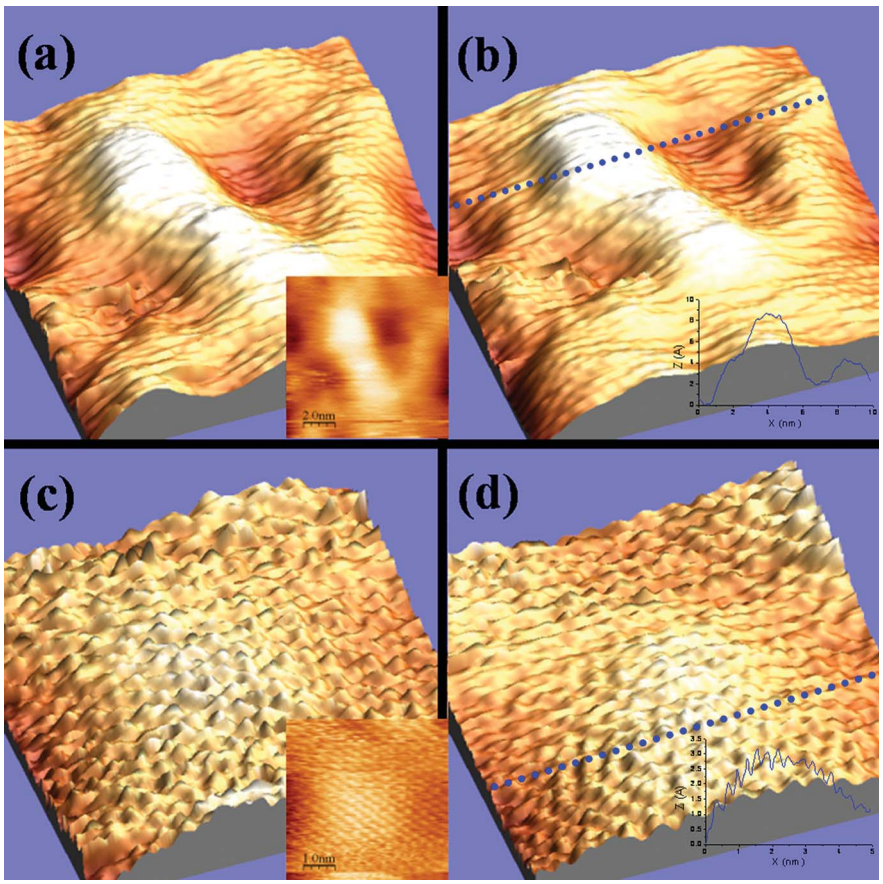

Fig. 4 High resolution 3D STM images of monolayer graphene. (a) First and (b) last image from an image series showing a 10 nm^2 area; (c) first and (d) last image from an image series showing a 5 nm^2 area. Both image pairs demonstrate that the ripples are static. The acquisition parameters were: $V_{bias} = +0.6$ V (tip bias) and $I = 0.5$ nA for (a) and (b) and +0.8 V and 0.6 nA for (c) and (d). Insets in (a) and (c) show the 2D counterparts. Insets in (b) and (d) show a line profile taken along the blue dotted lines.

Stolyarova *et al.*[2] and Ishigami *et al.*[4] have attributed such ripples to the interaction between graphene and the underlying substrate surface (in their case silicon dioxide) whose roughness may have led to corrugations with strong and defined patterns; they do not ascribe the ripples to intrinsic properties of graphene, in contrast to observations by Geringer *et al.*[16] However, in the absence of any substrate or support, our measurements on suspended graphene strongly suggest that the observed ripples are not related to substrate interactions so they might be formed *via* an interaction with the still present contamination or an intrinsic feature of graphene or as a result of the interaction between the tip and the graphene flake. However, the latter is unlikely because no change has been observed on the ripples appearances as is stated above. We can also eliminate ripple formation as a result of impurities left on graphene by scanning areas of tens of nm^2 where no contamination is observed. The ripples we observe in unsupported graphene are static in nature; the long term stability and reproducibility of the images and the ability to perform atomic resolution imaging both mitigate against a ripple structure which is varying on any time frame that would perturb STM imaging. Equally the bias polarity independence of our images strongly supports the view that topology rather than electronic image information is present in these images.

It is important to note that STM z-images are sensitive to both the surface local density of states (LDOS) variation and topology variation. The sensitivity of the STM tip response to each of these is a strong function of tip proximity and tunnelling current. The measurement conditions may be tuned to enhance sensitivity to electronic phenomena (electron density or LDOS magnitude) or to topology.[31] In general a high tunnelling current enhances LDOS sensitivity. Such considerations have been applied to STM imaging of graphene grown by CVD onto polycrystalline copper by Xu *et al.*[32] These workers optimised the LDOS imaging of filled states and showed that the high values of LDOS characteristic of graphene produced a near sinusoidal and unusually large *z* variation of the tip, with a spatial period of 0.25–3 nm and an amplitude of around 0.05 nm. This degree of tip displacement is a direct consequence of the unusually high density of filled states in graphene. The same sinusoidal ripple structure is seen in this work (Fig. 4(d)); it is the filled state LDOS response as the tip passes over each hexagonal benzene ring structure. However the gross ripple structure measured here corresponds to tip displacement around one order of magnitude greater than that resulting from the graphene LDOS and can only be assigned to topological variation in these unsupported films.

In conclusion, suspended graphene has been studied by STM for the first time. Annealing conditions have been established for imaging free-standing graphene membranes with atomic resolution and both monolayer and bilayer regions as well as ripples were observed. The ripples were stable over the entire measurement period, and hence appear to be static. The here established imaging conditions set the scene for future spectroscopic investigations of suspended graphene at low temperature in the STM (*I–V*), which are expected to provide a new experimental insight into intrinsic and fundamental properties of pristine graphene, through elimination of substrate and impurity effects.

Notes and references

1 A. T. N'Diaye, S. Bleikamp, P. J. Feibelman and T. Michely, *Phys. Rev. Lett.*, 2006, **97**, 215501.
2 E. Stolyarova, K. T. Rim, S. Ryu, J. Maultzsch, P. Kim, L. E. Brus, T. F. Heinz, M. S. Hybertsen and G. W. Flynn, *Proc. Natl. Acad. Sci. U. S. A.*, 2007, **104**, 9209–9212.
3 P. Mallet, F. Varchon, C. Naud, L. Magaud, C. Berger and J. Y. Veuillen, *Phys. Rev. B: Condens. Matter Mater. Phys.*, 2007, **76**, 041403.
4 M. Ishigami, J. H. Chen, W. G. Cullen, M. S. Fuhrer and E. D. Williams, *Nano Lett.*, 2007, **7**, 1643–1648.
5 K. Xu, P. Cao and J. R. Heath, *Nano Lett.*, 2009, **9**, 4446–4451.
6 G. Li, A. Luican and E. Y. Andrei, *Phys. Rev. Lett.*, 2009, **102**, 176804.
7 L. Gao, J. R. Guest and N. P. Guisinger, *Nano Lett.*, 2010, **10**, 3512–3516.
8 Z. Zhou, F. Gao and D. W. Goodman, *Surf. Sci.*, 2010, **604**, L31–L38.
9 K. S. Novoselov, A. K. Geim, S. V. Morozov, D. Jiang, Y. Zhang, S. V. Dubonos, I. V. Grigorieva and A. A. Firsov, *Science*, 2004, **306**, 666–669.
10 A. Reina, X. Jia, J. Ho, D. Nezich, H. Son, V. Bulovic, M. S. Dresselhaus and J. Kong, *Nano Lett.*, 2009, **9**, 30–35.
11 X. Li, W. Cai, J. An, S. Kim, J. Nah, D. Yang, R. Piner, A. Velamakanni, I. Jung, E. Tutuc, S. K. Banerjee, L. Colombo and R. S. Ruoff, *Science*, 2009, **324**, 1312–1314.
12 K. S. Kim, Y. Zhao, H. Jang, S. Y. Lee, J. M. Kim, K. S. Kim, J.-H. Ahn, P. Kim, J.-Y. Choi and B. H. Hong, *Nature*, 2009, **457**, 706–710.
13 C. Berger, Z. Song, X. Li, X. Wu, N. Brown, C. Naud, D. Mayou, T. Li, J. Hass, A. N. Marchenkov, E. H. Conrad, P. N. First and W. A. de Heer, *Science*, 2006, **312**, 1191–1196.
14 B. Premlal, M. Cranney, F. Vonau, D. Aubel, D. Casterman, M. M. De Souza and L. Simon, *Appl. Phys. Lett.*, 2009, **94**, 263115.
15 M. Sicot, S. Bouvron, O. Zander, U. Rudiger, Y. S. Dedkov and M. Fonin, *Appl. Phys. Lett.*, 2010, **96**, 093115.
16 V. Geringer, M. Liebmann, T. Echtermeyer, S. Runte, M. Schmidt, R. Rückamp, M. C. Lemme and M. Morgenstern, *Phys. Rev. Lett.*, 2009, **102**, 076102.
17 A. Luican, G. Li, A. Reina, J. Kong, R. R. Nair, K. S. Novoselov, A. K. Geim and E. Y. Andrei, *Phys. Rev. Lett.*, 2011, **106**, 126802.
18 J. C. Meyer, A. K. Geim, M. I. Katsnelson, K. S. Novoselov, T. J. Booth and S. Roth, *Nature*, 2007, **446**, 60–63.
19 R. Zan, U. Bangert, Q. Ramasse and K. S. Novoselov, *J. Microsc.*, 2011, **244**, 152–158.
20 F. Varchon, R. Feng, J. Hass, X. Li, B. N. Nguyen, C. Naud, P. Mallet, J. Y. Veuillen, C. Berger, E. H. Conrad and L. Magaud, *Phys. Rev. Lett.*, 2007, **99**, 126805.
21 G. Giovannetti, P. A. Khomyakov, G. Brocks, V. M. Karpan, J. van den Brink and P. J. Kelly, *Phys. Rev. Lett.*, 2008, **101**, 026803.
22 J. Wintterlin and M. L. Bocquet, *Surf. Sci.*, 2009, **603**, 1841–1852.
23 R. F. Egerton, P. Li and M. Malac, *Micron*, 2004, **35**, 399–409.
24 J. H. Warner, M. H. Rummeli, L. Ge, T. Gemming, B. Montanari, N. M. Harrison, B. Buchner and G. A. D. Briggs, *Nat. Nanotechnol.*, 2009, **4**, 500–504.
25 I. Horcas, R. Fernandez, J. M. Gomez-Rodriguez, J. Colchero, J. Gomez-Herrero and A. M. Baro, *Rev. Sci. Instrum.*, 2007, **78**, 013705–013708.
26 R. E. Peierls, *Ann. Inst. Henri Poincare*, 1935, **5**, 177–222.
27 L. D. Landau, *Phys. Z. Sowjetunion*, 1937, **11**, 26–35.
28 A. Fasolino, J. H. Los and M. I. Katsnelson, *Nat. Mater.*, 2007, **6**, 858–861.
29 T. J. Booth, P. Blake, R. R. Nair, D. Jiang, E. W. Hill, U. Bangert, A. Bleloch, M. Gass, K. S. Novoselov, M. I. Katsnelson and A. K. Geim, *Nano Lett.*, 2008, **8**, 2442–2446.
30 U. Bangert, M. H. Gass, A. L. Bleloch, R. R. Nair and J. Eccles, *Phys. Status Solidi A*, 2009, **206**, 2115–2119.
31 B. Hamilton, J. Jacobs and M. Missous, *J. Phys.: Condens. Matter*, 2003, **15**, S3083–S3093.
32 P. Xu, Y. Yang, S. D. Barber, M. L. Ackerman, J. K. Schoelz, I. A. Kornev, S. Barraza-Lopez, L. Bellaiche and P. M. Thibado, *Phys. Rev. B: Condens. Matter Mater. Phys.*, 2011, **84**, 161409.

